NEMESIS
Negative Effects in Medical Sciences Oral and Maxillofacial Surgery
UCL PRESSES UNIVERSITAIRES DE LOUVAIN

Three-dimensional analysis of airway space and mandibular morphology in Pierre Robin sequence using cone beam computed tomography.

Authors:
Olszewski R (DDS, MD, PhD, Prof)[1,*],
Dontaine T (MD, DDS)[1],
Odri GA (MD, PhD)[2],
Zech F (MD, PhD)[3],
Bayet B (MD)[4],
Reychler H (MD, DMD, Dhc, Prof)[1]

Affiliations:

[1] Department of oral and maxillofacial surgery, Cliniques universitaires saint Luc, Université catholique de Louvain, Brussels, Belgium
[2] Service de chirurgie orthopédique, CHU Lariboisière, Paris, France
[3] Department of Internal medicine, Cliniques universitaires saint Luc, Université catholique de Louvain, Brussels, Belgium

[4] Department of plastic surgery, Cliniques universitaires saint Luc, Université catholique de Louvain, Brussels, Belgium

Corresponding author: Olszewski R, Department of oral and maxillofacial surgery, Cliniques universitaires saint Luc, Université catholique de Louvain, Av. Hippocrate 10, 1200 Brussels, Belgium, raphael.olszewski@uclouvain.be; phone: +3227645718; fax number: +3227645876; ORCID iD: orcid.org/0000-0002-2211-7731

Disclaimer: the views expressed in the submitted article are our own and not an official position of the institution or funder.

Cover letter

Dear Editor-in-Chief,

Please receive our article titled "Three-dimensional analysis of airway space and mandibular morphology in Pierre Robin sequence using cone beam computed tomography" for open evaluation in Nemesis journal.

1) Summarize the study's contribution to the scientific literature: We developed, validated and applied a new three-dimensional (3D) cephalometric method of analysis to evaluate mandibular morphology in Pierre Robin sequence (PRS) patients. Our null hypothesis was that we would not find a significant difference between the PRS and control group patients in oropharyngeal airway volume measurements. Although the null hypothesis was confirmed, we found 3D morphological modifications of the mandibular vertical ramus in PRS patients who were not previously described in the literature. We also developed a reproducible method for 3D measurements of the superior airway space and applied it for the first time in PRS patients, compared to normal patients.

2) Relate the study to previously published work: there was no previous work on 3D cephalometric method of analysis to evaluate mandibular morphology in Pierre Robin sequence patients.

3) Specify the type of article (for example, research article, systematic review, meta-analysis, clinical trial): we provide with research article, and retrospective study.

4) Describe any prior interactions with Nemesis regarding the submitted manuscript: we have no prior interactions with Nemesis journal.

5) Nemesis aim and scope relevance: We worked on a rare disease (Pierre robin sequence). Our research shown that our null hypothesis was confirmed. Moreover we failed to find exactly the same control group under 9 years-old due to radioprotection restrictions on application of cone beam CT in children.

Abstract

Objectives: The Pierre Robin sequence (PRS) is defined by retromicrognathia, glossoptosis, and sleep apnea and can also be associated with cleft palate. Diagnosis, management and mandibular catch-up growth are still controversial issues in PRS patients. The aim of our retrospective study was to evaluate in three dimensions (3D) the airway space and mandibular morphology in PRS compared to a normal control group patients in the pre-orthodontic period of life. The null hypothesis was that we would not find a significant difference between the PRS and control group patients in oropharyngeal airway volume measurements. Material and methods: We analyzed 9 PRS patients (mean age: 8 years-old) who underwent cleft palate surgery in the first four months of life, performed by the same surgeon using the same technique. Cone-beam computed tomography (CBCT) was performed in these patients after local ethical committee approval. The control group consisted of 15 patients (mean age: 9 years-old) with CBCT already performed for other reasons. 3D Slicer was used in both groups for semi-automatic segmentation of the airway space. Two independent observers performed semi-automatic segmentations twice in each patient with a one- week interval between the two series of measurements. Airway volume was automatically measured using 3D Slicer. We also developed a 3D cephalometric analysis with Maxilim software in order to define a 3D mandibular morphology which consisted of 25 landmarks, 4 planes, and 23 distances. Two independent observers performed the 3D cephalometric analysis twice for each patient, with a one- week interval between the two series of measurements. Results: There was no significant difference in the intra- and inter-observer measurements between the PRS and control groups for airway space volume ($p<0.05$). However, there was a significant difference in the shape of the mandible between the PRS group and the control group ($p<0.05$). Conclusions: Vertical ramus width and mandibular global anteroposterior length were significantly lower in the PRS group. Mandibular hypoplasia could be found in PRS patients not only in the horizontal dimension. Nemesis relevance: the null hypothesis was confirmed. Moreover we failed to find exactly the same control group under 9 years-old due to radioprotection restrictions of application of cone beam CT in children.

Keywords: Pierre Robin syndrome, cone beam computed tomography, airways, segmentation, cephalometry, three-dimensional

Introduction

Pierre Robin sequence (PRS) is a consequence of clinical events that results from having a small mandible (retromicrognathia) [1]. The tongue becomes posteriorly displaced (glossoptosis) and obstructs airways (sleep apnea) [1-4]. Alternative proposed mechanisms of airway obstruction in PRS patients have included disproportionate tongue growth, tongue prolapse into the cleft palate, if present, lack of voluntary control of the tongue musculature, and negative pressure pulling the tongue into the hypopharynx [4, 5]. A small mandible can result from an inherent genetic growth problem or be deformational with a lack of mandibular catch-up growth when the intrauterine growth of the mandible has been restricted [1]. Controversies persist about mandibular "catch-up" growth in PRS patients [6]. Trying to resolve this controversy is important because it is related to the initial treatment of patients with small mandibles. Patients who were believed to experience "catch-up" growth of the mandible received tongue-lip adhesion or nasopharyngeal airway tubes as temporary measures [1]. Patients who were believed not to have experienced "catch-up" growth (syndromic patients) received early mandibular distraction osteogenesis which remains an invasive technique [1, 7].

Different modalities have been used to quantify micrognathia, glossoptosis, and airway obstruction [4, 8, 9]. Two-dimensional (2D) cephalometric studies have provided controversial evidence. Pruzansky and Richmond [10] used cephalograms to analyze mandibular shape and growth in children with micrognathia [11, 12], and they postulated that the mandible has significant potential for growth in children with PRS [13]. Poswillo [14] proposed that mandibular "catch-up" growth is likely to occur in deformational (intrauterine constriction) [15], but not in syndromic patients [1]. Figuroa et al.'s [16] used 2D cephalometry to determine the sizes, growth, and relationships of the mandible, tongue, and airway in isolated, non-syndromic PRS infants compared with normal and non-PRS cleft palate patients during first two years of age. Figuroa et al's [16] results supported the hypothesis of "partial mandibular catch-up growth" in PRS children. The increased growth rate in PRS patients improves airway dimensions, which might have been partly responsible for the natural resolution of respiratory distress. However, this increased growth rate did not allow for the various structures to reach values equal to normal [16]. In addition, other 2D cephalometric studies, using similar measurements and control groups, have postulated the absence of mandibular "catch-up" growth, persistence of small mandibles [4, 11, 15, 17-20], and convex profiles [11, 15, 18, 20, 21]. Finally, Krimmel et al, using 3D photogrammetry of the face [22] showed that sagittal deficits in the midface were present in non-syndromic PRS patients at birth and remained throughout active facial growth. For airway evaluation in PRS patients, Hermann et al [23] showed with 2D cephalometry, that the pharyngeal airway was reduced. However, Lenza et al [24] demonstrated that the upper airways could not

be accurately explored using single linear measurements as provided by 2D cephalometry. A cone-beam computed tomography (CBCT)-based three-dimensional (3D) analysis provides a better picture of the anatomical characteristics of the upper airway and therefore can result in an improvement of the diagnosis [24, 25]. PRS patients can also present with cleft palate. Recently Cheung et al [25] proved, using a 3D CBCT technique, that patients with cleft lip palate (CLP) did not exhibit smaller total airway volumes and cross-sectional areas than non-CLP controls [26]. Aras et al [27] also found that there were no differences between unilateral CLP patients and controls regarding nasopharyngeal airway volumes in 3D. Two-dimensional cephalometry appears to be the technique of choice to analyze the mandibular morphology and airway space in PRS patients [4, 11, 15, 17-20]. However, there is still a risk of error due to flaws in this radiological technique. The most common error arises from the choice of an insufficient distance between the source and target or from the application of an inadequate filter [28]. X-ray beam can also penetrate too much (or not enough) [28]. Opaque bodies of the cephalostat can overlap the anatomic structures of interest (e.g., mandibular condylar heads), or the patient's head can be wrongly oriented in the cephalostat [28, 29]. All 2D cephalometric analyses are based on the choice of specific reference landmarks on lateral or frontal radiography. The positioning of the majority of cephalometric reference landmarks is difficult as a result of the superposition of anatomic structures on lateral (or frontal) radiography. This difficulty is responsible for the low reproducibility of 2D cephalometrics [30-32]. Moreover, many reference landmarks, common to a majority of 2D cephalometric analyses, are not characterized by any anatomic reality [28]. For example, the "sella" reference landmark (the center of the sella turcica) is situated in an empty space at mid-distance of the segment of line linking the "posterior clinoid process" and "anterior clinoid process" landmarks. Some reference landmarks are also positioned at the intersections of radiological shadows, such as the "articulare" landmark (superposition of the shadow of the inferior border of the clivus and of the posterior limit of the mandibulary condyle) [28]. Finally, difficulty in quantifying right-left asymmetry on lateral radiography has also been recognized as a weakness of this technique [28, 29, 33].

The aim of our article was twofold: 1) to validate a 3D CBCT-based technique for measuring oropharyngeal airways in PRS patients, compared to a group of normal patients in a similar stage of growth; and 2) to validate a 3D CBCT-based cephalometric analysis in PRS patients, compared to a group of normal patients in a similar stage of growth. Following Cheung et al [26], our hypothesis was that we would not find a significant difference between the PRS and control group patients in oropharyngeal airway volume measurements. Concerning 3D CBCT mandibular cephalometry, our hypothesis was that we would not find a significant difference between the PRS and control group in 3D mandibular morphology.

Materials and methods

Materials

This study was a retrospective, case-control study based on CBCT data from consecutive patients with PRS who presented, with their parents, for follow-up consultation at the cleft lip and palate center of our university hospital. Written informed consent was obtained for all participants in the study, which was approved by our local ethical committee (no. B403201111247) [26]. For the PRS group, the inclusion criteria were white race, with glossoptosis, retromicrognathia and postero-median U-shaped cleft palates, and no associated syndromes. All PRS patients were within stage 1 according to Thibaut et al. (normal respiration, normal succion-deglutition, mild gastro-esophageal reflux, mild vagal hypertonia) [34]. All of the PRS patients received Veau-Wardill-Kilner pushback palatoplasty [35] at a mean age of 4 months old, performed by the same surgeon. The exclusion criteria were non-white race, syndromic patients, and non-compliance with CBCT examination (claustrophobia, movements inside the device, patients unable to understand the instructions). Finally, the PRS group consisted of 9 children, 6 girls and 3 boys, with a mean age of 8 years old. The control group consisted of consecutive patients retrieved retrospectively by birth date from a larger dentomaxillofacial CBCT database maintained by the department of medical imaging of our university hospital. CBCT examinations for the control group were performed for other reasons than the criteria for this study. The inclusion criteria were Caucasians with an age as close as possible to the mean age of the PRS group at the time of CBCT examination. The exclusion criteria consisted of non-Caucasians, patients with other cleft palate disorders or syndromes, diseases and/or malformations involving the mandible and/or the superior airway space, and CBCT examinations that were non-interpretable due to patient movement or metallic artifacts. Finally, the control group consisted of 15 patients, 9 girls and 6 boys, with a mean age of 9 years old.

Cone-beam computed tomography (CBCT) (iCAT®, Imaging Sciences International, Hatfield, PA, USA) was performed for all patients in the standard head position for visualization and quantification of the superior airway space and for evaluation of mandibular morphology.

Methods for superior airway volume measurements

3D Slicer open-source software (SPL, Harvard Medical School, USA) (http://www.slicer.org) was used for semi-automatic segmentation of the superior airway space on CBCT images in both groups (Fig. 1) [36-39].

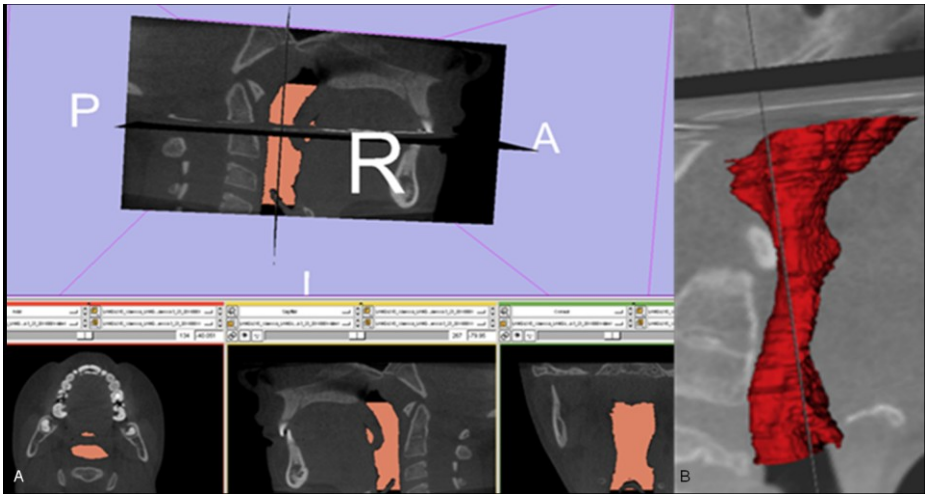

Fig. 1 A. Segmentation of the airway space with 3D slicer software in control group patient. B. Three-dimensional reconstruction of airway space in PRS group patient.

The superior limit of segmentation was the palate at the level of the posterior nasal spine. The inferior limit of segmentation was parallel to the superior limit of segmentation and was the last axial slice passing through the osseous mandibular chin. Two independent observers performed semi-automatic segmentations twice in each patient with a one-week interval between the two series of segmentations. The observers were not aware of the patient group allocation (PRS or control group) when they performed the segmentation. Airway volume (in mm^3) was automatically measured with 3D Slicer software.

Statistical method for superior airway volume measurements

Normal distribution was tested with the Kolmogorov-Smirnoff test. Means were compared using a two-way unpaired t test. Intra- and inter-observer reproducibility were analyzed by the intra-class correlation coefficients (ICC 2.1 model: two way random single measurements for absolute agreement) [40, 41]. The inter-observer results were analyzed separately in the control group and in the PRS group. All the tests were performed using SPSS® for Widows, version 16.0. The difference was considered significant when $p<0.05$.

Methods for the development of 3D cephalometric analysis

We developed a new 3D cephalometric analysis technique for the evaluation of mandibular morphology which consisted of 15 landmarks identified directly on 3D CBCT mandibular reconstructions, 4 planes, 9 constructed landmarks belonging to planes, one constructed landmark as a mid-point between two landmarks, and 23 distance measurements. First, we tested the reproducibility for the 15 non-constructed landmarks identified directly on 3D CBCT mandibular reconstructions. The parameters for the 3D CBCT clinical protocol were 120 kV, 36.9 mA, 40 ms, a 160 x 130 mm field of view and a reconstruction voxel of 0.3 mm. The scanning limits for 3D CBCT were from the chin to the level of the upper glenoid fossa. All native data were saved on CD (DICOM format), and 3D reconstructions were performed with Maxilim software (Medicim, Leuven, Belgium). The 3D surface rendering was based on the marching cubes algorithm [42]. Two experienced oral and maxillofacial surgeons participated in this study as independent observers. Each of the observers identified and used a mouse to indicate manually 15 non-constructed landmarks on each 3D surface rendering (Table 1, Figures 2-6).

Table 1. Landmarks and planes: definitions.

Landmarks on 3D CBCT reconstructions	**Definition**
1. Canine (right, left)	Mid-position at the vestibular face of the mandibular canine crown at the level of alveolar crest
2. Condyle (right, left)	Most upper and posterior point on the mandibular condyle
3. Coronoid process (right, left)	Top of the coronoid process
4. First molar (right, left)	Mid-position at the lingual face of the 1st mandibular molar crown at the level of alveolar crest
5. Gonion (right, left)	Most convex point of the mandibular angle
6. Inter-incisive	Vestibular alveolar crest between first mandibular incisors
7. Lingula (right, left)	Top of the lingula
8. Sigmoid notch (right, left)	Most concave point of the sigmoid notch
Planes	
1. Inter-incisive-bi-lingula	Plane based on 3 landmarks: "inter-incisive",

	"lingula right", "lingula left"
2. Vertical molar	Plane based on two landmarks "1st molar right", "1st molar left", and perpendicular to plane inter-incisive bi-lingula
3. Vertical canine	Plane based on two landmarks "canine right", "canine left", and perpendicular to plane inter-incisive bi-lingula
4. Sagittal plane	Plane based on one landmark "inter-incisive" and perpendicular to plane inter-incisive bi-lingula and to plane vertical molar
Landmarks on planes	
1. Notch anterior (right, left)	Intersection between plane inter-incisive-bi-lingula and anterior vertical ramus of the mandible
2. Notch posterior (right, left)	Intersection between plane inter-incisive-bi-lingula and posterior vertical ramus of the mandible
3. Basilar molar (right, left)	Intersection between plane vertical molar and horizontal ramus of the mandible (the most convex point at the level of basilar mandible)
4. Basilar canine (right, left)	Intersection between plane vertical canine and horizontal ramus of the mandible (the most convex point at the level of basilar mandible)
5. Basilar inter-incisive	Intersection between sagittal plane and osseous chin (the most convex point at the level of mandibular symphysis)
Landmarks as a mean of 2 landmarks	
1. Mid-lingula	Mid-landmark between lingula right and lingula left

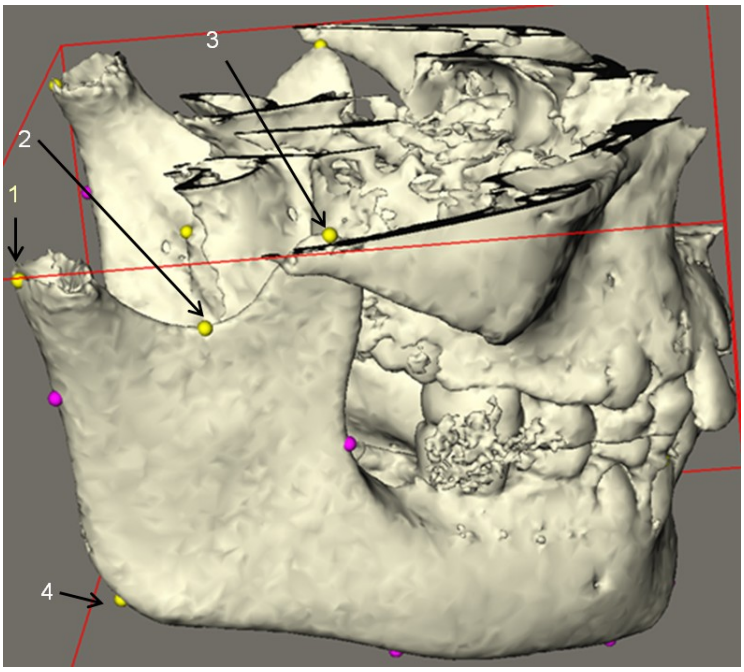

Fig. 2 Landmarks on 3D CBCT reconstruction, right lateral view: 1) condyle right, 2) sigmoid notch right, 3) coronoid process right, 4) gonion right.

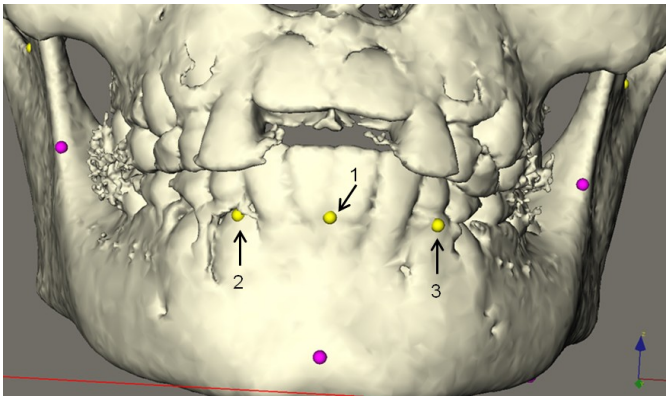

Fig. 3 Landmarks on 3D CBCT reconstruction, frontal view: 1) inter-incisive, 2) canine right, 3) canine left.

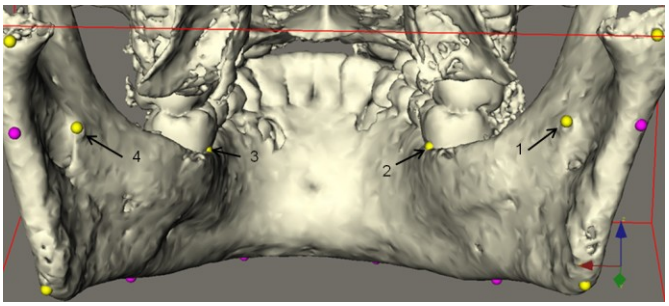

Fig. 4 Landmarks on 3D CBCT reconstruction, posterior-anterior view: 1) lingula right, 2) 1st molar right, 3) 1st molar left, 4) lingula left.

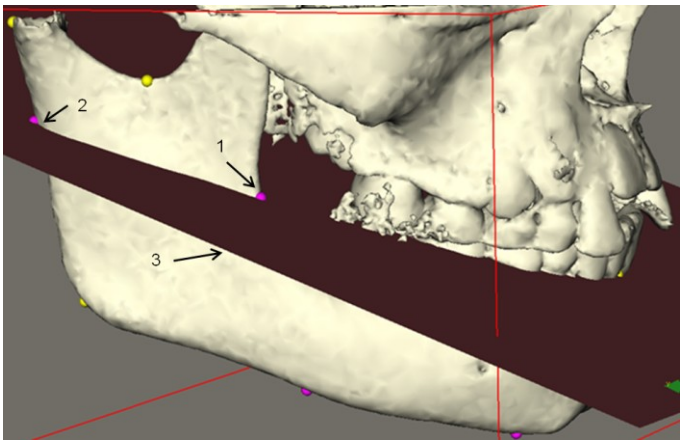

Fig. 5 Landmarks on planes, right lateral view: 1) Notch anterior right, 2) Notch posterior right, 3) Plane inter-incisive-bi-lingula.

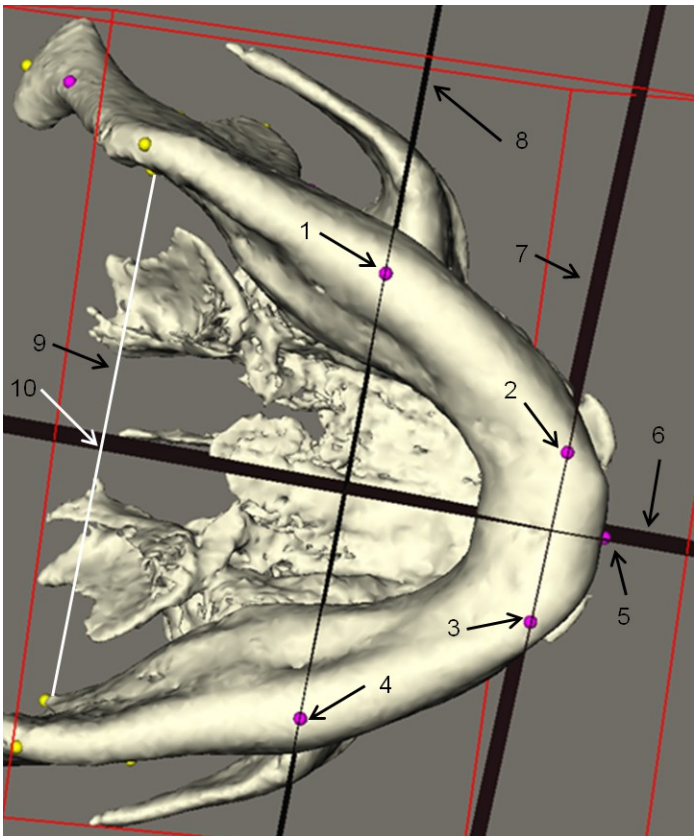

Fig. 6 Landmarks on planes, inferior view: 1) Basilar molar right, 2) Basilar canine right, 3) Basilar canine left, 4) Basilar molar left, 5) Basilar inter-incisive, 6) Sagittal plane, 7) Vertical canine plane, 8) Vertical molar plane, 9) distance mid-lingula, 10) mid-lingula.

Seven bilateral landmarks ("canine", "condyle", "coronoid process", "first molar", "gonion", "lingula", and "sigmoid notch") and one unilateral midline landmark ("inter-incisive") were identified. Each observer performed two series of landmark identifications for both protocols, in all 24 patients. The observations were performed with a one-week interval between them. The observers were not aware of the patient group allocation (PRS or control group) when they identified the landmarks. The 3D coordinates (x, y, and z) for each cranial landmark were automatically saved with Maxilim software.

Statistical analysis methodology for landmark reproducibility

The observers evaluated the positions of 15 anatomic cephalometric landmarks for each mandible and for each method in 3D space. To estimate the accuracy of the two methods, we focused on the reproducibility of the positioning of an anatomical landmark in 3D space. The actual position of each identified landmark was unknown. We posited that the measured landmarks were normally distributed (i.e., formed a Gaussian distribution), with a standard deviation of "s" in 3D space with regard to the actual position of the landmark. We did not hypothesize about the actual position of the landmark to be measured, instead simply calculating the distances between measured landmarks with regard to the observer (inter-observer) and the observation (intra-observer). However, when measured landmarks were distant from actual landmarks with a normally distributed (a Gaussian distribution) error, the mean of the distances between the measured and actual landmarks was equal to the mean of the distances between successive measurements of measured landmarks divided by 1.221. To estimate the distance of measurements with regard to position of the actual landmark, all of the values in the tables had to be divided by 1.221. The mean distances between the successive measurements in 3D space were directly related to "s" according to the following formula:

$$\text{mean distance} = \int_0^{\infty}\int_0^{\infty}\int_{-1}^{1} \sqrt{y^2 + z^2 - 2.y.z.k}\, \frac{e^{-\frac{y^2}{2.s^2}}.e^{-\frac{z^2}{2.s^2}}}{\pi.s^2} \quad \partial k\, \partial y\, \partial z = 1.221 s$$

where s = mean distance/1.221.

The standard error of the mean distances was 0.7134 s. All of the values listed in the tables had to be divided by 1.221 to provide estimations of the standard deviations of the dispersion around the actual positions of the landmarks. The distances between localizations of the same landmark were based on linear regression by generalized estimating equations (GEE), using quasi-likelihood estimation [43]. For gamma-distribution data, the canonical link for the dependent variable y as a function of the independent parameter x, was an inverse negative relationship, $y = -1/(\beta_0 + \beta_1.x_1 + \beta_2.x_2 \ldots)$, for data presenting a variance proportional to the square of the mean. We computed the covariance matrix by the quasi-least-squares method (QLS) [44] because the values were most likely correlated for the same mandible and the same landmark. All of the intra-observer and inter-observer distances were incorporated into a common regression [45].

Statistical methodology for distance measurements between 3D cephalometric landmarks

Normality and statistical tests were performed using SPSS® for Windows, version 16.0. Student's independent t test was applied on the interobserver results. The same method was used to test the PRS group compared to the control group.

Results

Superior airway space volume measurements for both observers (intra- and inter-observer) and for both groups (control and PRS) are presented in Tables 2-4. Intra-observer and inter-observer intraclass correlation coefficients (ICC) for the control and PRS groups are presented in Tables 5 and 6. To evaluate the reproducibility of 3D cephalometric non-constructed landmarks, the parameters studied in the regression were: 1) control and syndromic groups ("group"); 2) anatomical landmarks ("landmark"); and 3) intra- and inter-observer measurements ("inter"). In the first step, we tested the interactions between "group" and "landmark" ($p=0.91$, NS) and between "group" and "inter" ($p=0.19$, NS). As there were no significant interactions in the first step, we were able to test the interactions between "group" ($p=0.0023$*), between "landmark" ($p<0.0000001$**), and between "inter" ($p<0.0000001$**). To measure the intra-observer harmonic mean distances in both groups (control and PRS), we used two (for one unilateral landmark) or four (for each of the seven bilateral landmarks) distances measured for each site and each mandible. Because we studied 24 patients, there were a total of 720 measurements performed. For measurement of the inter-observer harmonic mean distances in both groups (control and PRS), we used four (for one unilateral landmark) or eight (for each of the seven bilateral landmarks) distances measured for each site and each mandible. Because we studied 24 patients, there were a total of 1440 measurements performed. The intra-observer and inter-observer harmonic mean distances for both groups are presented in Tables 7 and 8. The harmonic mean distances between two measurements for the 15 tested mandibular landmarks are presented in Table 9. Finally, 23 distance measurements between 3D cephalometric landmarks in the control and PRS groups are presented in Table 10.

345 **Table 2.** Intra-observer airway space volume measurements in control and
346 PRS group.

Control and PRS groups (N=24)	Observer n°1 (1st observation)	Observer n°1 (2nd observation)	Observer n°2 (1st observation)	Observer n°2 (2nd observation)
Mean	14308.48	13921.72	14642.81	14559.98
SD*	4403.71	4345.44	4723.54	4541.15
SEM**	898.90	887.01	964.18	926.95
p	0.76 NS		0.95 NS	

347
348 Measurements are in mm^3 (significant if $p<0.05$).
349 SD*: standard deviation, SEM**: standard error of the mean
350

351 **Table 3.** Inter-observer airway space volume measurements in control and
352 PRS group.

	Control group (N=15)		**PRS group (N=9)**	
	Observer n°1	Observer n°2	Observer n°1	Observer n°2
Mean	14290.97	15032.22	13821.98	13883.35
SD	4796.79	5058.86	3755.65	3884.60
SEM	1238.52	1313.16	1251.88	1294.86
p	0.68 NS		0.97 NS	

353 Measurements are in mm^3 (significant if $p<0.05$)
354

355 **Table 4.** Comparison between airway space volume measurements in
356 control and PRS group.

	Control group (N=15)	**PRS group (N=9)**
Mean	14661.60	13852.67
SD	4929.64	3807.33
SEM	1272.82	1269.11
p	0.67 NS	

357

Table 5. Intra-observer intraclass correlation coefficients (ICC) for control and PRS group.

	Control group		**PRS group**	
	1st observer	2nd observer	1st observer	2nd observer
ICC	0.996	0.998	0.938	0.956

Table 6. Inter-observer intraclass correlation coefficients (ICC) for control and PRS group.

	Control group	**PRS group**	**Control and PRS groups**
	Mean 1st/2nd observer	Mean 1st/2nd observer	Mean 1st/2nd observer
ICC	0.979	0.987	0.980

Table 7. Intra-observer harmonic means and their confidence interval at 95%.

	Control group	**PRS group**
Harmonic mean	0.895	0.831
95 % confidence interval	0.831-0.962	0.750-0.920

Table 8. Inter-observer harmonic means and their confidence interval at 95%.

	Control group	**PRS group**
Harmonic mean	1.174	1.003
95 % confidence interval	1.105-1.248	0.928-1.083

371 **Table 9.** Harmonic mean distances and their confidence interval at 95 %
372 for manually identified landmarks.

Landmark name	Harmonic mean distance	Confidence interval at 95 %
Canine	0.985	0.857-1.131
Condyle	1.590	1.429-1.774
Coronoid process	0.771	0.660-0.897
First molar	0.705	0.602-0.822
Gonion	1.650	1.489-1.833
Inter-incisive	0.539	0.413-0.689
Lingula	1.051	0.954-1.159
Sigmoid notch	0.714	0.625-0.813

373

374 **Table 10.** Mean distance measurements in mm (significant if p<0.05).

	Control group Observer n°1/observer n°2	**PRS group Observer n°1/ Observer n°2**	**Control group/PRS group**
1. Basilar canine left basilar inter-incisive	Mean Obs1=16.43 Mean Obs2=16.60 p=0.84 NS	Mean Obs1=16.30 Mean Obs2=15.60 p=0.69 NS	Mean control=16.51 Mean PRS=15.95 p=0.65 NS
2. Basilar canine right basilar inter-incisive	Mean Obs1=16.38 Mean Obs2=16.62 p=0.81 NS	Mean Obs1=16.86 Mean Obs2=17.58 p=0.73 NS	Mean control=16.50 Mean PRS=17.22 p=0.62 NS
3. Basilar molar left basilar canine left	Mean Obs1=38.54 Mean Obs2=39.01 p=0.84 NS	Mean Obs1=35.76 Mean Obs2=35.75 p=0.98 NS	Mean control=38.78 Mean PRS=35.75 p=0.18 NS
4. Basilar molar right basilar canine right	Mean Obs1=39.26 Mean Obs2=38.81 p=0.85 NS	Mean Obs1=31,90 Mean Obs2=33.33 p=0.35 NS	Mean control=39.03 Mean PRS=32.61 p=0.05*
5. Bi-canine	Mean Obs1=24.77 Mean Obs2=24.07 p=0.63 NS	Mean Obs1=25.97 Mean Obs2=24.65 p=0.68 NS	Mean control=24.42 Mean PRS=25.31 p=0.67 NS
6. Bi-condyle	Mean Obs1=90.98 Mean Obs2=90.68 p=0.82 NS	Mean Obs1=92.12 Mean Obs2=89.86 p=0.29 NS	Mean control=90.83 Mean PRS=90.99 p=0.92 NS
7. Bi-gonial	Mean Obs1=84.38 Mean Obs2=84.11 p=0.89 NS	Mean Obs1=84.08 Mean Obs2=83.79 p=0.88 NS	Mean control=84.24 Mean PRS=83.93 p=0.88 NS
8. Bi-lingula	Mean Obs1=73.13 Mean Obs2=73.22 p=0.93 NS	Mean Obs1=71.43 Mean Obs2=71.72 P=0.82 NS	Mean control=73.18 Mean PRS=71.58 p=0.22 NS

9. Bi-molar	Mean Obs1=66.95 Mean Obs2=65.28 p=0.41 NS	Mean Obs1=68.97 Mean Obs2=66.75 p=0.25 NS	Mean control=66.11 Mean PRS=67.86 p=0.41 NS
10. Bi-sigmoid	Mean Obs1=88.88 Mean Obs2=88.71 p=0.89 NS	Mean Obs1=87.41 Mean Obs2=87.22 p=0.88 NS	Mean control=90.30 Mean PRS=89.27 p=0.26 NS
11. Gonion left basilar molar left	Mean Obs1=27.18 Mean Obs2=30.72 p=0.23 NS	Mean Obs1=23.63 Mean Obs2=32.60 p=0.02*	Mean control=28.95 Mean PRS=28.11 p=0.78 NS
12. Gonion left condyle left	Mean Obs1=48.75 Mean Obs2=45.10 p=0.03*	Mean Obs1=42.47 Mean Obs2=39.02 p=0.40 NS	Mean control=46.92 Mean PRS=40.75 p=0.001*
13. Gonion left coronoid process left	Mean Obs1=53.45 Mean Obs2=52.24 p=0.16 NS	Mean Obs1=48.43 Mean Obs2=47.28 p=0.47 NS	Mean control=52.85 Mean PRS=47.86 p=0.0002**
14. Gonion right basilar molar right	Mean Obs1=26.20 Mean Obs2=30.86 p=0.05*	Mean Obs1=21.39 Mean Obs2=32.21 p=0.013*	Mean control=28.53 Mean PRS=26.80 p=0.49 NS
15. Gonion right condyle right	Mean Obs1=48.18 Mean Obs2=44.34 p=0.003**	Mean Obs1=46.67 Mean Obs2=41.32 p=0.005*	Mean control=46.29 Mean PRS=43.99 p=0.09 NS
16. Gonion right coronoid process right	Mean Obs1=53.21 Mean Obs2=51.64 p=0.15 NS	Mean Obs1=49.88 Mean Obs2=48.28 p=0.37 NS	Mean control=52.42 Mean PRS=49.08 p=0.018*
17. Mid-lingula inter-incisive	Mean Obs1=63.92 Mean Obs2=63.87 p=0.98 NS	Mean Obs1=54.58 Mean Obs2=54.98 p=0.85 NS	Mean control=63.90 Mean PRS=54.78 p=0.0003**
18. Notch anterior left sigmoid left	Mean Obs1=28.03 Mean Obs2=29.00 p=0.30 NS	Mean Obs1=29.53 Mean Obs2=30.72 p=0.63 NS	Mean control=28.51 Mean PRS=30.13 p=0.13 NS
19. Notch anterior-posterior left	Mean Obs1=37.87 Mean Obs2=37.97 p=0.92 NS	Mean Obs1=35.69 Mean Obs2=35.76 p=0.93 NS	Mean control=37.92 Mean PRS=35.72 p=0.049*
20. Notch anterior-posterior right	Mean Obs1=37.62 Mean Obs2=37.77 p=0.87 NS	Mean Obs1=35.60 Mean Obs2=35.81 p=0.81 NS	Mean control=37.69 Mean PRS=35.70 p=0.05*
21. Notch anterior right sigmoid right	Mean Obs1=27.31 Mean Obs2=28.46 p=0.30 NS	Mean Obs1=30.88 Mean Obs2=31.42 p=0.51 NS	Mean control=27.89 Mean PRS=31.15 p=0.005**
22. Notch posterior left sigmoid left	Mean Obs1=19.25 Mean Obs2=19.69 p=0.59 NS	Mean Obs1=16.61 Mean Obs2=17.18 p=0.50 NS	Mean control=19.47 Mean PRS=16.89 p=0.007*
23. Notch posterior right sigmoid right	Mean Obs1=18.94 Mean Obs2=19.17 p=0.72 NS	Mean Obs1=16.90 Mean Obs2=17.53 p=0.51 NS	Mean control=19.05 Mean PRS=17.21 p=0.026**

375

376

Discussion

Airway volume measurements with 3D Slicer software was a reproducible method (Tables 2-6) between control and PRS groups. We found that there were no significant differences in oropharyngeal airway volume measurements between the control and PRS patients, and therefore, our initial hypothesis was accepted. Our results were in agreement with the 3D study by Cheung et al [26]. However, we did not compare airway volumes between different anatomical levels such as the nasopharynx, oropharynx, and hypopharynx [26]. Additionally, we did not include nasal cavity volume measurements in our study. The nasal cavity has a much more complicated anatomy to segment than the oropharyngeal airway; therefore, our study might over-represent the true validity of the evaluated method [41]. The respiratory cycle was not controlled while the scans were obtained. However, respiration is a dynamic action that cannot be accurately depicted on the static 3D images we used [26]. Finally, we did not correlate our volume results with dental occlusion types (classes of Angle I, II, and III), as done by Cheung et al [26], because only the shape of the airway is modified according to dental occlusion class and not the volume itself [46].

Concerning the reproducibility of the 15 non-constructed landmarks, the method used was at least as good in the PRS group as in the control group (Tables 7 and 8). PRS condition did not affect the difficulty of identifying and positioning the landmarks on 3D CBCT skull reconstructions. We did not test the reproducibility of 10 other constructed landmarks because their positions were dependent on the initial positioning of the 15 non-constructed landmarks. Some landmarks, such as the "gonion" and "condyle", were less reproducible than the other landmarks chosen for this study (Table 9). The "gonion" landmark lies on a convex and smooth angle of the mandible. The "condyle" landmark lies on a smooth and convex area of the mandibular condyle. Identification of the "condyle" landmark might also have been more difficult due to partial ossification and, therefore, worse 3D reconstruction of the mandibular condyle in the pre-orthodontic stage. Therefore, we discarded all measurements involving the "gonion" and "condyle" landmarks when comparing the PRS and control groups using 3D morphological analysis of the mandible (distance nos. 11-16, Table 10, supplementary Tables 1-3). There were no significant differences between the PRS and control groups concerning transversal (right-left) mandibular distances (distances nos. 5-10, Table 10). However, we found a significant difference between the PRS and control groups regarding global anterior-posterior distances (distance no. 17, Table 10, supplementary Tables 1-3, Figure 7), with a significant tendency toward global micrognathia in the PRS group.

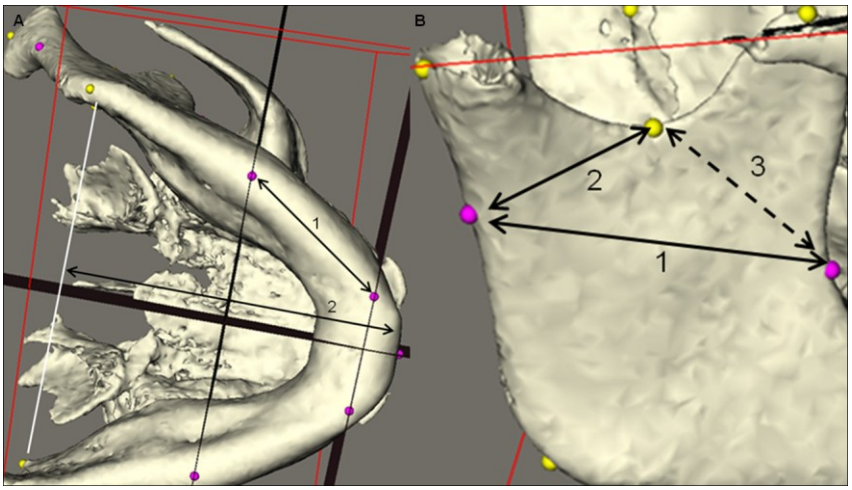

Fig. 7 A. Mandibular inferior view. Significantly increased distances in control compared to PRS group: 1) distance basilar canine-basilar molar right, 2) distance mid-lingula-inter-incisive. B. Right mandibular lateral view. Significantly increased distances in control compared to PRS group 1) notch anterior-notch posterior, 2) sigmoid notch-notch posterior; significantly increased distances in PRS compared to control group: 3) notch anterior-sigmoid notch.

We also found that the horizontal body of the mandible was significantly shorter in the anterior-posterior direction on the right side of the mandible (distance no. 4, Table 10, supplementary Tables 1-3, Figure 7). We found a significant difference between the PRS and control groups concerning the anterior-posterior distances of the vertical ramus (distance nos. 19 and, 20, Table 10, supplementary Tables 1-3, Figure 7) with a significant tendency toward anteroposterior hypoplasia of the vertical ramus in the PRS group. However, we found that the neck of the coronoid process was significantly larger unilaterally in the PRS group, compared to the control group (distance no. 21, Table 10, supplementary Tables 1-3, Figure 7). We found that the neck of the mandibular condyle was significantly larger in the control group, compared to the PRS group (distance nos. 22 and, 23, Table 10, supplementary Tables 1-3). Some tendency toward mandibular asymmetry on the same side was revealed in the PRS group using our 3D morphological analysis at the level of the horizontal mandibular body and of the coronoid process [47]. Due to the lack of reproducibility of the "gonion" and "condyle" landmarks, we cannot provide reproducible measurements for the posterior vertical height of the vertical ramus in the PRS and control groups [48]. Finally, our initial hypothesis, about not significant

differences between the PRS and control groups in mandibular morphology, was rejected.

The main limitation of our retrospective, case-control study was the limited number of PRS patients and non-perfect matching between the groups on the base of age. We could not find a lot of CBCT examinations for control patients with ages younger than 9 years-old because of the exponential risk of thyroid cancer in young patients [49]. However, between the ages of 8 and 9 years–old, a relative stagnation in children's mandibular growth occurs [50]. This stagnation could explain that not all of the mandibular distances from PRS patients were significantly smaller compared to the control group. In conclusion, we validated two reproducible methods for: 1) the measurement of oropharyngeal airway volume; and 2) 3D mandibular morphology evaluation in PRS patients. We showed that mandibular hypoplasia could be found in PRS patients not only in the horizontal dimension [51]. Insertions of masticatory muscles lie on the neck of the coronoid process (temporal muscle), the neck of mandibular condyle (pterygoid muscle) and the anteroposterior width of vertical ramus (masseter muscle). Therefore, further investigation should be directed toward evaluation of the volume and function of the masticatory muscles of the mandible (masseter, temporal, pterygoid) in PRS patients comparatively to control groups, to explain better the morphological findings of our study. Finally, more PRS patients must be included in a larger study to provide more complete evidence regarding the absence of "catch-up" growth.

- **Acknowledgements**: none.
- **Funding sources statement**: this study does not receive any funding.
- **Competing interests**: Prof Raphael Olszewski is Editor-in-chief of NEMESIS journal. All other authors declare that they have no competing interests related to this study.

Compliance with ethical standards

- **Conflict of Interest**: The authors declare that they have no conflict of interest.
- **Ethical approval**: "All procedures performed in studies involving human participants were in accordance with the ethical standards of the institutional and/or national research committee and with the 1964 Helsinki declaration and its later amendments or comparable ethical standards."
- **Informed consent**: "Informed consent was obtained from all individual participants included in the study."

475 **Authors contribution:**

Author	Contributor role
Olszewski R	Conceptualization, Investigation, Methodology, Project administration, Resources, Supervision, Validation, Visualization, Writing original draft preparation, Writing-review and editing
Dontaine T	Investigation, Methodology, Formal analysis, Validation, Writing-review and editing
Odri GA	Methodology, Formal analysis, Writing original draft preparation, Writing-review and editing
Zech F	Methodology, Formal analysis, Writing-review and editing
Bayet B	Resources (surgery), Writing-review and editing
Reychler H	Supervision, Writing-review and editing

476

477 ## References

478 1. Mackay DR. Controversies in the diagnosis and management of the Robin
479 sequence. J Craniofac Surg 2011;22:415-420.

480 2. Robin P. A drop of the base of the tongue considered as a new cause of
481 nasopharyngeal respiratory impairment [in French]. Bull Acad Natl Med (Paris)
482 1923;89:37–41.

483 3. Robin P. A fall of the base of the tongue considered as a new cause of
484 nasopharyngeal respiratory impairment: Pierre Robin sequence, a translation—
485 1923. Plast Reconstr Surg 1994;93:1301–1303.

4. Evans KN, Sie KC, Hopper RA, Glass RP, Hing AV, Cunningham ML. Robin Sequence: From Diagnosis to Development of an Effective Management Plan. Pediatrics 2011;127:936–948.

5. Mallory SB, Paradise JL. Glossoptosis revisited: on the development and resolution of airway obstruction in the Pierre Robin syndrome. Pediatrics 1979;64:946–948.

6. Chowchuen B, Jenwitheesuk K, Chowchuen P, Prathanee B. Pierre Robin sequence: challenges in the evaluation, management and the role of early distraction osteogenesis. J Med Assoc Thai 2011;94:S91-S99.

7. Genecov DG, Barceló CR, Steinberg D, Trone T, Sperry E. Clinical experience with the application of distraction osteogenesis for airway obstruction. J Craniofac Surg 2009;20:1817-1821.

8. van der Haven I, Mulder JW, van der Wal KG, Hage JJ, de Lange-de Klerk ES, Haumann TJ. The jaw index: new guide defining micrognathia in newborns. Cleft Palate Craniofac J 1997;34:240–241.

9. Vegter F, Hage JJ, Mulder JW. Pierre Robin syndrome: mandibular growth during the first year of life. Ann Plast Surg 1999;42:154–157.

10. Pruzansky S, Richmond JB. Growth of mandible in infants with micrognathia: clinical implications. Am J Dis Child 1954;88:29–42.

11. Laitinen SH, Heliovaara A, Ranta RE. Craniofacial morphology in young adults with the Pierre Robin sequence and isolated cleft palate. Acta Odontol Scand 1997;55:223–228.

12. Pradel W, Lauer G, Dinger J, Eckelt U. Mandibular traction: an alternative treatment in infants with Pierre Robin sequence. J Oral Maxillofac Surg 2009;67:2232–2237.

13. Pruzansky S. Not all dwarfed mandibles are alike. Birth Defects Orig Artic Ser 1969;2:120–129.

14. Poswillo D. The aetiology and pathogenesis of craniofacial deformity. Development 1988;103:207–212.

15. Suri S, Ross RB, Tompson BD. Mandibular morphology and growth with and without hypodontia in subjects with Pierre Robin sequence. Am J Orthod Dentofacial Orthop 2006;130:37-46.

16. Figueroa AA, Glupker TJ, Fitz MG, BeGole EA. Mandible, tongue, and airway in Pierre Robin sequence: a longitudinal cephalometric study. Cleft Palate Craniofac J 1991;28:425–434.

17. Daskalogiannakis J, Ross RB, Tompson BD. The mandibular catch-up growth controversy in Pierre Robin sequence. Am J Orthod Dentofacial Orthop 2001;120:280–285.

18. Laitinen SH, Ranta RE. Cephalometric measurements in patients with Pierre Robin syndrome and isolated cleft palate. Scand J Plast Reconstr Hand Surg 1992;26:177–183.

19. Eriksen J, Hermann NV, Darvann TA, Kreiborg S. Early postnatal development of the mandible in children with isolated cleft palate and children with nonsyndromic Robin sequence. Cleft Palate Craniofac J 2006;43:160-167.

20. Shen Y, Vargervik K, Oberoi S, Chigurupati R. Facial skeletal morphology in growing children with Pierre Robin sequence. Cleft Palate Craniofac J 2012;49:553-560.

21. Ozawa TO, Lorenzoni DC, de Oliveira LG, da Silva Filho OG. Facial profile evaluation of isolated pierre robin sequence. Cleft Palate Craniofac J 2012;49:546-552.

22. Krimmel M, Kluba S, Breidt M, Bacher M, Dietz K, Buelthoff H, Reinert S. Three-dimensional assessment of facial development in children with Pierre Robin sequence. J Craniofac Surg 2009;20:2055-2060.

23. Hermann NV, Kreiborg S, Darvann TA, Jensen BL, Dahl E, Bolund S. Craniofacial morphology and growth comparisons in children with Robin Sequence, isolated cleft palate, and unilateral complete cleft lip and palate. Cleft Palate Craniofac J 2003;40:373-396.

24. Lenza MG, Lenza MM, Dalstra M, Melsen B, Cattaneo PM. An analysis of different approaches to the assessment of upper airway morphology: a CBCT study. Orthod Craniofac Res 2010;13:96-105.

25. Ghoneima A, Kula K. Accuracy and reliability of cone-beam computed tomography for airway volume analysis. Eur J Orthod 2013;35:256-261.

26. Cheung T, Oberoi S (2012) Three dimensional assessment of the pharyngeal airway in individuals with non-syndromic cleft lip and palate. PLoS One 7:e43405

27. Aras I, Olmez S, Dogan S (2012) Comparative evaluation of nasopharyngeal airways of unilateral cleft lip and palate patients using 3 dimensional and 2 dimensional methods. Cleft Palate Craniofac J 49:e75-81

28. Bouvart B (1980) Les analyses céphalométriques. Etude critique et comparative. Rev Stomatol Chir Maxillofac [in French] 81:201-224

29. Delaire J (1984) Quelques pièges dans les interprétations des téléradiographies céphalométriques. Rev Stomatol Chir Maxillofac [in French] 85:176-185

30. Da Silveira HL, Silveira HE (2006) Reproducibility of cephalometric measurements made by three radiology clinics. Angle Orthod 76:394-399

31. Houston WJB, Maher RE, McElroy D, Sherriff M (1986) Sources of error in measurements from cephalometric radiographs. Eur J Orthod 8:149-151

32. Ongkosuwito EM, Katsaros C, van t'Hof MA, Bodegom JC, Kuipers-Jagtman AM (2002) The reproducibility of cephalometric measurements: a comparison of analogue and digital methods. Eur J Orthod 24:655-665

33. Olszewski R, Reychler H (2004) Limitations of orthognathic model surgery: theoretical and practical implications. Rev Stomatol Chir Maxillofac [in French] 105:165-169

34. Thibault C, Vernel-Bonneau F (1999) Les fentes facials: embryologie, rééducation, accompagnement parental. Masson, Paris

35. Leow AM, Lo LJ (2008) Palatoplasty: evolution and controversies. Chang Gung Med J 31:335-345

36. Pieper S, Lorensen B, Schroeder W, Kikinis R (2006) The NA-MIC Kit: ITK, VTK, Pipelines, Grids and 3D Slicer as an Open Platform for the Medical Image Computing Community. Proceedings of the 3rd IEEE International Symposium on Biomedical Imaging: From Nano to Macro 1:698-701

37. Pieper S, Halle M, Kikinis R (2004) 3D SLICER. Proceedings of the 1st IEEE International Symposium on Biomedical Imaging: From Nano to Macro 1:632-635

38. Gering D, Nabavi A, Kikinis R, Grimson W, Hata N, Everett P, Jolesz F, Wells W (1999) An Integrated Visualization System for Surgical Planning and Guidance using Image Fusion and Interventional Imaging. Int Conf Med Image Comput Comput Assist Interv 2:809-819

39. Fedorov A, Beichel R., Kalpathy-Cramer J, Finet J, Fillion-Robin J-C, Pujol S, Bauer C, Jennings D, Fennessy F, Sonka M, Buatti J, Aylward SR, Miller JV, Pieper S., Kikinis R (2012) 3D Slicer as an Image Computing Platform for the Quantitative Imaging Network. Magnetic Resonance Imaging 30:1323-1341

40. Shrout PE, Fleiss JL (1979) Intraclass correlations: uses in assessing rater reliability. Psychol Bull 86:420-428

589 41. Alsufyani NA, Flores-Mir C, Major PW (2012) Three-dimensional
590 segmentation of the upper airway using cone beam CT: a systematic review.
591 Dentomaxillofac Radiol 41:276-284

592 42. Lorensen WE, Cline HE (1987) Marching cubes: a high resolution 3D surface
593 construction algorithm. Comp Graph 21:163-169

594 43. McCullagh P (1983) Quasi-likelihood functions. Ann Stat 11:59-67

595 44. Chaganty NR, Shults J (1999) On eliminating the asymptotic bias in the quasi-
596 least squares estimate of the correlation parameter. J Stat Plan Inf 76:145-161

597 45. Olszewski R, Reychler H, Cosnard G, Denis JM, Vynckier S, Zech F (2008)
598 Accuracy of three-dimensional (3D) craniofacial cephalometric landmarks on
599 low-dose 3D computed tomography. Dentomaxillofac Radiol 37:261-267

600 46. Grauer D, Cevidanes LS, Styner MA, Ackerman JL, Proffit WR (2009)
601 Pharyngeal airway volume and shape from cone-beam computed tomography:
602 relationship to facial morphology. Am J Orthod Dentofacial Orthop 136:805-
603 814

604 47. Mulder CH, Kalaykova SI, Gortzak RA (2012) Coronoid process hyperplasia: a
605 systematic review of the literature from 1995. Int J Oral Maxillofac Surg
606 41:1483-1489

607 48. Chang EI, Clemens MW, Garvey PB, Skoracki RJ, Hanasono MM (2012)
608 Cephalometric analysis for microvascular head and neck reconstruction. Head
609 Neck 34:1607-1614

610 49. Ronckers CM, Sigurdson AJ, Stovall M, Smith SA, Mertens AC, Liu Y,
611 Hammond S, Land CE, Neglia JP, Donaldson SS, Meadows AT, Sklar CA,
612 Robison LL, Inskip PD (2006) Thyroid cancer in childhood cancer survivors: a
613 detailed evaluation of radiation dose response and its modifiers. Radiat Res
614 166:618-628

615 50. Coquerelle M, Prados-Frutos JC, Benazzi S, Bookstein FL, Senck S,
616 Mitteroecker P, Weber GW (2013) Infant growth patterns of the mandible in
617 modern humans: a closer exploration of the developmental interactions between
618 the symphyseal bone, the teeth, and the suprahyoid and tongue muscle insertion
619 sites. J Anat 222:178-192

620 51. Lu DW, Shi B, Wang HJ, Zheng Q (2007) The comparative study of
621 craniofacial structural characteristic of individuals with different types of cleft
622 palate. Ann Plast Surg 59:382-387

623